ORIGINAL RESEARCH COMMUNICATION

Title:

Real-time imaging of the bacillithiol redox potential in the human pathogen *Staphylococcus aureus* using a genetically encoded bacilliredoxin-fused redox biosensor

Authors:

Vu Van Loi[1], Manuela Harms[2], Marret Müller[3], Nguyen Thi Thu Huyen[1], Chris J. Hamilton[4], Falko Hochgräfe[2], Jan Pané-Farré[3] and Haike Antelmann[1]*

Departments & Institutions:

[1]*Institute for Biology-Microbiology, Freie Universität Berlin, D-14195 Berlin, Germany*

[2]*Junior Research Group Pathoproteomics and* [3]*Institute for Microbiology,*
Ernst-Moritz-Arndt-University of Greifswald, D-17487 Greifswald, Germany

[4]*School of Pharmacy, University of East Anglia, Norwich Research Park, Norwich, NR4 7TJ, UK*

Abbreviated title: Bacilliredoxin-fused redox biosensor in *Staphylococcus aureus*

*Corresponding author:

Haike Antelmann, Institute for Biology-Microbiology, Freie Universität Berlin,

Königin-Luise-Strasse 12-16, D-14195 Berlin, Germany,

Tel: +49-(0)30-838-51221, Fax: +49-(0)30-838-451221

E-mail: haike.antelmann@fu-berlin.de

Key words: *Staphylococcus aureus*/ bacillithiol/ bacilliredoxin/ redox biosensor

Word count:	**6004**
Number of references:	**41**
Number of greyscale images:	**4**
Number of colour images:	**2**

SUMMARY

Aims: Bacillithiol (BSH) is utilized as major thiol-redox buffer in the human pathogen *Staphylococcus aureus*. Under oxidative stress, BSH forms mixed disulfides with proteins, termed as *S*-bacillithiolation which can be reversed by bacilliredoxins (Brx). In eukaryotes, glutaredoxin-fused roGFP2 biosensors have been applied for dynamic live-imaging of the glutathione redox potential. Here, we have constructed a genetically encoded bacilliredoxin-fused redox biosensor (Brx-roGFP2) to monitor dynamic changes in the BSH redox potential in *S. aureus*. ***Results:*** The Brx-roGFP2 biosensor showed a specific and rapid response to low levels bacillithiol disulphide (BSSB) *in vitro* which required the active-site Cys of Brx. Dynamic live-imaging in two methicillin-resistant *S. aureus* (MRSA) USA300 and COL strains revealed fast and dynamic responses of the Brx-roGFP2 biosensor under hypochlorite and H_2O_2 stress and constitutive oxidation of the probe in different BSH-deficient mutants. Furthermore, we found that the Brx-roGFP2 expression level and the dynamic range is higher in *S. aureus* COL compared to the USA300 strain. In phagocytosis assays with THP-1 macrophages, the biosensor was 87 % oxidized in *S. aureus* COL. However, no changes in the BSH redox potential were measured after treatment with different antibiotics classes indicating that antibiotics do not cause oxidative stress in *S. aureus*. ***Conclusion and Innovation:*** This Brx-roGFP2 biosensor catalyzes specific equilibration between the BSH and roGFP2 redox couples and can be applied for dynamic live imaging of redox changes in *S. aureus* and other BSH-producing Firmicutes.

INTRODUCTION

Staphylococcus aureus is an opportunistic human pathogen causing local skin infections, but also life-threatening diseases like septicemia, endocarditis and necrotizing pneumoniae (1,3,21). The success of the pathogen is mediated by virulence factors and by the development of multiple antibiotic resistant *S. aureus* strains, such as methicillin-resistant isolates (MRSA) (19). *S. aureus* has to cope with oxidative stress by reactive oxygen species (ROS), such as H_2O_2 and the strong oxidant hypochloric acid by the oxidative burst of macrophages and neutrophils under infection conditions (41). As defense mechanisms, *S. aureus* uses various redox-sensing virulence regulators and the thiol-redox-buffer bacillithiol (BSH) (5,13,20,28,30,32-34). BSH functions in detoxification of ROS, hypochlorite, diamide, methylglyoxal, electrophiles and antibiotics, such as rifampicin and fosfomycin or heavy metal ions and protects *S. aureus* against the oxidative burst by activated macrophages in phagocytosis assays (10,20,32,33). Under hypochlorite stress, BSH forms mixed disulfides with proteins (*S*-bacillithiolations) as a widespread thiol-protection and redox-switch mechanism analogous to *S*-glutathionylation in eukaryotes (6,7,17,20). In *B. subtilis*, two glutaredoxin-like enzymes YphP (BrxA) and YqiW (BrxB) with unusual CGC motifs were characterized as bacilliredoxins **(Figures 1A and S1)** that catalyze the reduction of *S*-bacillithiolated proteins, leading to formation of bacillithiolated Brx (Brx-SSB) as intermediate of this bacilliredoxin electron pathway (9). Reduction of Brx-SSB requires BSH resulting in BSSB formation that could be recycled by the putative BSSB reductase (YpdA) on expense of NADPH **(Figure 1B)** (9,10,12,20).

The standard thiol-redox potential of BSH was calculated as $E^{0'}$(BSSB/BSH) = -221mV which is higher than the glutathione redox potential [$E^{0'}$(GSSG/GSH) = -240 mV] (31,36). To date, all previous studies have used fluorescent bimane-labelling of thiols for quantification of BSH and BSSB levels by high-pressure liquid chromatography (HPLC) under control and stress conditions as indicator of the changes in the BSH redox potential. According to this method, the BSH/BSSB ratios range from 100:1 to 400:1 in *B. subtilis,* suggesting that BSH is mostly present in its reduced form (36). Under conditions of *S*-bacillithiolation provoked by NaOCl stress, the level of BSSB increases indicating a more oxidized BSH redox potential (7). However, the applied methods require disruption of cells and do not allow dynamic measurements of the changes in the BSH redox potential (25,35). Thus, recent

advances in the design of genetically encoded redox biosensors, such as redox sensitive green fluorescent proteins (roGFPs) have facilitated the real-time imaging of the cellular redox potential without cell disruption and at high sensitivity under *in vivo* conditions (11,24,35). These roGFP biosensors allow the ratiometric measurements based on two excitation maxima at 405 and 488 nm that change upon oxidation (24,25). RoGFP2 was fused to human glutaredoxin to construct the Grx-roGFP2 biosensor for real-time measurements of dynamic changes in the GSH redox potential (E_{GSH}) in different compartments and different eukaryotic organisms. Grx-roGFP2 detects nanomolar concentrations of GSSG against a backdrop of millimolar GSH within seconds (11,24). Recently, roGFP-based biosensors were applied in pathogenic organisms to study E_{GSH} changes under infection conditions and antibiotic treatment, including the malaria parasite *Plasmodium falciparum* (15) and the Gram-negative bacterium *Salmonella* Typhimurium (38,39)*.* In malaria parasites, several antimalarial drugs affected the cellular redox metabolism and showed differential responses of the Grx-roGFP2 biosensor under short- and long-term measurements *in vivo* (15)*.* In *Mycobacterium tuberculosis,* an analogous Mrx1-roGFP2 biosensor was developed for dynamic measurements of the mycothiol redox potential (E_{MSH}) in drug-resistant isolates and inside macrophages (2,24). The Mrx1-roGFP2 biosensor was applied to screen for new ROS-generating anti-TB drugs that affected E_{MSH} (37).

In this study, we have constructed the first bacilliredoxin-fused roGFP biosensor that is highly specific to measure changes of the BSH redox potential in methicillin-resistant *Staphylococcus aureus* (MRSA) strains USA300 and COL under oxidative stress and following infection of THP-1 human macrophage-like cells.

Results

Construction of a Brx-roGFP2 biosensor that is highly specific for BSSB. The thioredoxin-fold proteins of the UPF0403 family YphP and YqiW were characterized as bacilliredoxins (BrxA and BrxB) in *B. subtilis* that function in reduction of *S*-bacillithiolated proteins and share an unusual CGC active site motif **(Figure 1A)** (9). Both Brx were *S*-bacillithiolated at their active site Cys *in vivo* and *in vitro* to form Brx-SSB during their catalytic cycle (9). Blast searches identified two bacilliredoxin homologs

4

in *S. aureus* USA300 (SAUSA300_1321 and SAUSA300_1463). SAUSA300_1321 showed 54 % sequence identity with YphP while SAUSA300_1463 shared stronger sequence identity (68 %) with YqiW of *B. subtilis* **(Figure S1)**. We selected the YphP-homolog SAUSA300_1321 (renamed Brx) for construction of a Brx-roGFP2 fusion protein. *S. aureus* Brx and Brx Cys-Ala-mutant proteins (BrxA$_{54}$GC$_{56}$, BrxC$_{54}$GA$_{56}$, BrxA$_{54}$GA$_{56}$) were each fused via the 30aa glycine-serine linker (11) to the N-terminus of roGFP2 to construct the Brx-roGFP2 biosensor variants. Analogous to the reaction of Grx1-roGFP2 and Mrx1-roGFP2 with GSSG or MSSM (2,24), oxidation of the Brx-roGFP2 biosensor should occur specifically by BSSB that targets the active site Cys54 of Brx to form Brx-SSB. This leads to the transfer of the BSH moiety to the coupled roGFP2 forming *S*-bacillithiolated roGFP2 which re-arranges to the roGFP2 disulfide resulting in ratiometric changes of the excitation maxima at 405 and 488 nm **(Figure 1C)**.

The His-tagged Brx-roGFP2 protein was expressed in *E. coli,* purified and compared to roGFP2 for its ratiometric changes in the fully reduced and oxidized forms using the microplate reader. The thiol-reactive oxidant diamide was used for complete oxidation and the thiol-reducing compound DTT was applied for complete reduction of the biosensor. Similar to roGFP2, Brx-roGFP2 exhibits two excitation maxima at 405 and 488 nm and responds in a ratiometric manner to 5 mM diamide and 10 mM DTT (2,24) **(Figure 1DE)**. The degree of oxidation (OxD) was calculated according to the fluorescence excitation intensities at 405 nm and 488 nm of fully oxidized and reduced Brx-roGFP2 probes as described previously (11). For all following measurements the OxD values of fully reduced and oxidized probes were calibrated as 0 and 1 and the OxD of the actual measurements were related to these controls. Furthermore, it was analysed if the Brx-roGFP2 response is sensitive by pH changes that could occur during infections. The Brx-roGFP2 probe was diluted into phosphate buffer solutions at different pH values ranging from 5.8 to 8.0 and treated with diamide and DTT **(Figure S2).** The 405/488 nm excitations ratios were not affected by different pH values indicating that the probe is insensitive to pH changes.

Purified Brx-roGFP2 showed a very fast and specific response to physiological BSSB levels (10-100 µM), but not to other thiol disulfides (GSSG, MSSM, cystine and CoAS disulfide) **(Figure 2AB).** In contrast, roGFP2 did not respond to 10-100 µM BSSB confirming that Brx-roGFP2 is specific

to detect E_{BSH} changes **(Figure 2C)**. Furthermore, Grx-roGFP2 was oxidized specifically by 100 µM GSSG, but was unresponsive to BSSB indicating that Grx is not specific for the BSH/BSSB redox couples (11) **(Figure 2D)**.

The specificity of Brx for BSSB should be determined by the $C_{54}GC_{56}$ active site motif. Hence, the response of Brx-roGFP2 was compared with that of Brx Cys mutant roGFP2 fusions where the active site Cys54 and the resolving Cys56 of Brx are each replaced by an alanine (BrxAGC, BrxCGA, BrxAGA). While Brx-roGFP2 and the resolving Brx Cys56 mutant (BrxCGA-roGFP2) showed very fast oxidation by 10-100 µM BSSB, the BrxAGC-roGFP2 and BrxAGA-roGFP2 active site mutant proteins failed to respond to 10 µM BSSB and showed weaker responses to 100 µM BSSB **(Figure 2EF)**. In previous studies, the BSH content was determined as 0.5-1.6 µmol/g raw dry weight (rdw) in BSH-producing *S. aureus* strains (36). This equates to 0.5-1.6 mM intracellular BSH assuming a 50% water content of the cellular biomass as determined for related bacteria (4). The BSH/BSSB ratio was estimated as 1:20-1:40 (28,32) indicating that the physiological BSSB content should be below 100 µM in *S. aureus*. Thus, the Brx-roGFP2 biosensor is highly specific to detect physiological levels of 10-100 µM BSSB *in vitro*.

Response of Brx-roGFP2 in *S. aureus* MRSA strains COL and USA300 along the growth curve and effect of BSH deficiency on the biosensor response. To monitor the changes in E_{BSH} inside *S. aureus*, Brx-roGFP2 was expressed ectopically from plasmid pRB473 under control of a xylose-inducible promoter in two MRSA isolates COL and USA300. The *S. aureus* wild type strains were grown in LB medium overnight with xylose and the strong roGFP2 fluorescence could be monitored using the microplate reader and fluorescence microscopy. First, we confirmed the ratiometric response of the Brx-roGFP2 biosensor inside *S. aureus* cells in the fully oxidized and reduced state after treatment with 5 mM diamide and 10 mM DTT, respectively and monitored the changes at the 405 and 488 nm excitation maxima **(Figure 3AB)**. Western blot analyses confirmed that Brx-roGFP2 is expressed as full-length protein and not degraded during the growth in *S. aureus* **(Figure S3)**. Next, the changes of the BSH redox potential were monitored during different stages of growth in LB medium in *S. aureus* **(Figure 3C-E)**. In fact, the expression and fluorescence intensity of Brx-roGFP2 varied

between the *S. aureus* COL and USA300 wild type strains along the growth. While a significant Brx-roGFP2 fluorescence signal was detected in *S. aureus* COL already during the exponential growth, the expression and fluorescence of Brx-roGFP2 were much weaker in *S. aureus* USA300 during the log phase **(Figure 3CD, Figure S4AB)**. In both strains, the oxidation degree of the Brx-roGFP2 increased during the stationary phase reflecting growth-dependent redox changes **(Figure 3E)**. Furthermore, we observed that the dynamic range of the 405/488 nm ratios of fully reduced and oxidized Brx-roGFP2 was higher in COL (3.77 ± 0.65) compared to USA300 (2.37 ± 0.98) **(Figure 3F)**. However, we confirmed that the level of Brx-roGFP2 did not affect the OxD since serial dilutions of *S. aureus* cells that were harvested at an OD of 4.0 showed the same OxD level **(Figure S4CD)**. Based on the oxidation degree of the biosensor, the intracellular BSH redox potential was calculated using the Nernst' equation, ranging from -300 to -270 mV in COL and from -300 to -235 mV in USA300 during exponential growth until transition into the stationary phase **(Table S5).**

We further compared biosensor oxidations between COL and USA300 wild types and isogenic BSH deficient mutants. The biosensor was fully oxidized in the COL and USA300 *bshA* mutants indicating an impaired redox balance and increased oxidative stress in the *bshA* mutant **(Figure 3GH)**. This constitutive biosensor oxidation was also observed in strain RN4220 which is a natural *bshC* mutant of the *S. aureus* NCTC8325 lineage (27,32,33) **(Figure S5).** Western blot analyses confirmed that the biosensor is similarly expressed in the COL wild type and *bshA* mutant **(Figure S6).**

Response of Brx-roGFP2 in *S. aureus* COL to oxidative stress. The changes in E_{BSH} were further investigated in *S. aureus* COL wild type in response to oxidative stress, provoked by H_2O_2 and NaOCl. Previous studies have shown that NaOCl stress leads to *S*-bacillithiolation of proteins and a decreased BSH/BSSB redox ratio (7). Since *S. aureus* is extremely resistant to H_2O_2 (14,40), the physiological sub-lethal concentrations of oxidants were determined **(Figure 4AB).** In addition, the role of BSH for the resistance to NaOCl and H_2O_2 was analyzed in survival assays. The *bshA* mutant was more sensitive than the wild type to 150 µM NaOCl and 300 mM H_2O_2 indicating that BSH contributes to oxidative stress resistance. The change in E_{BSH} after exposure to 1-100 mM H_2O_2 and 10-100 µM NaOCl and the time for detoxification of oxidants and recovery of the reduced state were investigated.

The biosensor was rapidly and reversibly oxidized by 10-50 mM H_2O_2 and cells approached a more reduced state within 70 minutes **(Figure 4C)**. Remarkably, 100 mM H_2O_2 did not result in complete oxidation of the biosensor (e.g. OxD = 1), although *S. aureus* cells were unable to restore their reduced state. Treatment of cells with low doses of 10-20 µM NaOCl resulted in reversible biosensor oxidation and required 200 min for regeneration of the reduced state. The biosensor was fully oxidized by 100 µM NaOCl, but cells were unable to recover **(Figure 4D)**. Using non-reducing BSH-specific Western blot analysis we further confirmed that 100 µM NaOCl stress leads to the same increase of *S*-bacillithiolated proteins in *S. aureus* COL and COL Brx-roGFP2 strains indicating that Brx-roGFP2 expression did not affect the *S*-bacillithiolation pattern **(Figure S7)**.

To analyse the impact of Brx in the biosensor response to the oxidants *in vivo*, attempts were made to express also unfused roGFP2 in *S. aureus* COL. However, in contrast to the Brx-roGFP2 fusion, expression of unfused roGFP2 failed in *S. aureus* COL containing the pRB473-roGFP2 plasmid. Thus, we compared the biosensor responses of the various Brx Cys mutant fusions (BrxAGC, BrxCGA, BrxAGA) to the different oxidants *in vivo*. The response of Brx-roGFP2 and BrxCGA-roGFP2 to 50 mM H_2O_2 was fast and reversible with recovery of the reduced state after 120 min. In contrast, oxidation of the Brx active site Cys mutant fusions (BrxAGC and BrxAGA) by H_2O_2 was slower and not fully reversible **(Figure 4E)**. We further analysed the responses of the BrxAGC, BrxCGA and BrxAGA Cys mutant fusions to 20 µM NaOCl. While all Brx Cys mutants responded similar to NaOCl, the BrxAGA double Cys mutant was unable to recover after 120 min **(Figure 4F)**. This indicates that a direct response of Brx-roGFP2 to high doses of 50 mM H_2O_2 and to the strong oxidant NaOCl could in part account for the oxidant responses in the absence of the CGC motif of Brx. To monitor the direct biosensor response to the oxidants, purified roGFP2 and Brx-roGFP2 proteins were both treated with different concentrations of H_2O_2 and NaOCl **(Figure S8)**. The results showed, that roGFP2 and Brx-roGFP2 both respond strongly to 1-10 mM H_2O_2 and 50-100 µM NaOCl leading to complete biosensor oxidation. This confirms that the Brx-roGFP2 biosensor could also directly respond to high H_2O_2 doses and the strong oxidant NaOCl *in vivo* in the absence of the Brx CGC motif. Another possibility could be that the third conserved Cys of Brx at the C-terminus (Cys144) is *S*-bacillithiolated by BSSB *in vivo* in the absence of the CGC motif leading to subsequent biosensor oxidation.

Confocal laser scanning microscopy of Brx-roGFP2 fluorescence in *S. aureus* COL wild type and Δ*bshA* mutant cells. The redox-dependent changes of Brx-roGFP2 fluorescence in *S. aureus* COL wild type and *bshA* mutant cells were analyzed using confocal laser scanning microscopy before and after NaOCl stress. The biosensor fluorescence intensities were measured after excitation at 405 nm and 488 nm and false-coloured in red and green, respectively **(Figure 5)**. The oxidation state of the biosensor is visualized by overlay of both red and green images. Confocal imaging showed that Brx-roGFP2 is reduced in non-treated wild type cells and resembles that of DTT-treated reduced cells with bright fluorescence at the 488 nm excitation wavelength **(Figures 5)**. NaOCl stress leads to a decreased fluorescence intensity of the 488 nm excitation maximum and strongly increased fluorescence at the 405 nm excitation maximum as shown in the histograms. Thus, NaOCl-treated wild type cells are visualized as red cells in the overlay images similar to the fully oxidized wild type control. In the *S. aureus* COL *bshA* mutant the Brx-roGFP2 biosensor was fully oxidized under control conditions as shown by the strong fluorescence in the 405 nm (red) channel which resembles the NaOCl-treated sample. The redox state of wild type and *bshA* mutant cells was calculated from five representative single cells and also using measurements in the microplate reader for comparison **(Figures 5 CD)**.

Response of Brx-roGFP2 in *S. aureus* following internalization by THP-1 macrophages. Next, we measured the changes in E_{BSH} of *S. aureus* under infection-like conditions during phagocytosis assays with activated THP-1 macrophages. Infection assays were performed with *S. aureus* COL cells at a multiplicity of infection (MOI) of 25 and fluorescence excitation intensities were monitored at 405 and 488 nm. After 1 hour of infection with *S. aureus* COL about 70-80 % of THP-1 cells showed a green fluorescence. As fully oxidized and reduced controls, infected macrophages were treated with 150 μM NaOCl and 20 mM DTT, respectively and the mean fluorescence intensity (MFI) at 405 and 488 nm was analysed using flow cytometry **(Table S7)**. The 405/488 nm ratio of the MFI of fully reduced and oxidized THP-1 controls was calibrated to 0% and 100% oxidation and related to the 405/488 nm ratio of the MFI of infected macrophages. In comparison to these fully reduced and

oxidized THP-1 controls, the biosensor was 87 % oxidized in *S. aureus* COL during infection following uptake by macrophage-like cells **(Table S7)**.

Effects of antibiotics on the Brx-roGFP2 biosensor response in *S. aureus* COL. We were interested in the changes of the BSH redox potential in response to sub-lethal antibiotics commonly used to treat MRSA infections. The aim was to clarify a long debate about the involvement of oxidative stress in the killing mode of antibiotics (16,18). We have chosen antibiotics with different cellular target sites, including RNA polymerase inhibitors (rifampicin), cell-wall biosynthesis inhibitors (fosfomycin, ampicillin, oxacillin and vancomycin), aminoglycosides as protein biosynthesis inhibitors that target the ribosome (gentamycin, lincomycin, erythromycin and linezolid), as well as fluoroquinolones (ciprofloxacin) that inhibits the DNA gyrase and topoisomerase IV to block DNA replication. *S. aureus* COL with Brx-roGFP2 was treated with sub-lethal concentrations of antibiotics and analyzed for its biosensor response. The sub-lethal antibiotics doses that caused a reduced growth rate were determined as 0.1 µM erythromycin, 0.1 µM rifampicin, 5 µM vancomycin, 30 µM ciprofloxacin, 0.5 µg/ml gentamicin, 10 µM ampicillin, 50 mM fosfomycin, 5 µM lincomycin, 2 µg/ml linezolid and 2 mM oxacillin. The measurement of the Brx-roGFP2 response revealed no increased biosensor oxidation by any of these antibiotics compared to the untreated control **(Figure 6, Table S6)**. These results document that sub-lethal antibiotics do not cause changes in the BSH redox potential in *S. aureus*.

DISCUSSION

Redox-sensitive GFPs have been recently fused to glutaredoxin and mycoredoxin for dynamic measurements of the intracellular redox potential in eukaryotes and Mycobacteria in real-time and at high sensitivity and spatiotemporal resolution (35). Here, we coupled the bacilliredoxin (Brx) to roGFP2 to measure the intracellular bacillithiol (BSH) redox potential in *S. aureus* cells under infection conditions, ROS and antibiotics treatments. This Brx-roGFP2 biosensor is highly sensitive and specific for physiological levels of BSSB while unfused roGFP2 and the BrxAGC active site mutant roGFP2 fusion are much lower responsive to BSSB *in vitro*. The role of the active site Cys of Brx for reduction

of S-bacillithiolated OhrR and MetE has been shown previously for *B. subtilis* BrxA and BrxB (9). The specific reaction of the active site Cys54 with BSSB was verified here for the *S. aureus* Brx homolog SAUSA300_1321 in the Brx-roGFP2 fusion. Thus, coupling of roGFP2 with the Brx facilitates rapid equilibration of the biosensor with the BSH/BSSB redox pair to selectively measure changes in the BSH redox potential. However, weaker responses of the BrxAGC and BrxAGA active site and double mutants were observed by 100 µM BSSB which could depend on the third C-terminal Cys144 residue that is also conserved across the UPF0403-family of Brx-homologs **(Figure S1)**.

The Brx-roGFP2 biosensor was applied to monitor the changes in the BSH redox potential inside the archaic HA-MRSA isolate COL and the CA-MRSA strain USA300. In both MRSA strains, BSH is required for survival under oxidative stress and infection-related conditions during phagocytosis with macrophages (32,33). Here, we confirmed that BSH-deficient mutants of *S. aureus* COL and USA300 are more sensitive to H_2O_2 and NaOCl compared to the wild types. We further monitored the perturbations in the BSH redox potential during growth, oxidative challenge and infection assays with THP-1 macrophages. Increases in E_{BSH} were observed in *S. aureus* COL and USA300 strains during the stationary phase in LB medium compared to the log phase. However, we confirmed that the expression level of Brx-roGFP2 did not affected the OxD **(Figure S4 CD)**. The dynamic range of Brx-roGFP2 was lower in USA300 compared to COL which could depend on the 1.6-fold higher BSH levels in USA300 (32). Differences in the basal level oxidation and dynamic range were also observed between drug-sensitive (3D7) and resistant (Dd2) *Plasmodium falciparum* parasites (15). In *P. falciparum* 3D7, the lower basal oxidation degree of the biosensor could be explained by the higher GSH levels. Thus, the higher BSH levels in USA300 could result in higher reducing capacity and lower biosensor response to diamide.

We further showed that the Brx-roGFP2 biosensor in *S. aureus* COL responds rapidly to ROS, such as H_2O_2 and NaOCl. However, *S. aureus* is resistant to high levels of 300 mM H_2O_2 (40). Thus, treatment of *S. aureus* with 1-10 mM H_2O_2 resulted only in a slightly increased biosensor oxidation with rapid regeneration of the reduced state. Exposure to 50-100 µM NaOCl stress caused the complete and constitutive oxidation of the biosensor and correlates with the observed *S*-bacillithiolation of proteins and increased levels of BSSB under NaOCl stress in *S. aureus* (7). The

comparison of the biosensor response of Brx-roGFP2 with that of the Brx Cys mutant fusion revealed similar response but changes in the recovery after H_2O_2 and NaOCl stress which was impaired in the Brx active site mutants. Thus, the biosensor could also directly respond to the high H_2O_2 levels and the strong oxidant NaOCl *in vivo*. The changes in BSH redox potential were also measured inside *S. aureus* COL during phagocytosis assays in THP-1 macrophage cell lines. The flow cytometric data showed that the Brx-roGFP2 biosensor was 87 % oxidized in *S. aureus* COL under infection conditions.

The comparison of the biosensor response in *S. aureus* COL and USA300 wild types and the isogenic *bshA* mutants as well as in the natural *bshC*-deficient strain RN4220 revealed a constitutive oxidation of the probe in the absence of BSH. This high biosensor oxidation in BSH-deficient strains is visualized also by confocal imaging at the cellular level. These results are in agreement with the constitutive oxidation of the Grx-roGFP2 biosensor upon GSH depletion in *Arabidopsis thaliana* seeds (23). Thus, our data clearly document the impaired redox balance in the absence of BSH and its major role to keep the reduced state of the cytoplasm in *S. aureus* cells. In addition to BSH depletion, much lower NADPH levels were previously measured in the Δ*bshA* mutant which could contribute to the impaired thiol-redox balance (32). In *S. aureus*, coenzyme A and Cys were suggested to function as alternative thiol-redox buffers and *S. aureus* encodes also a CoAS disulfide reductase to keep CoASH in the reduced state (22). However, based on the microscopic and macroscopic pK_a values of BSH, the level of the reactive thiolate anion is much higher in BSH compared to CoASH and Cys at physiological pH values (36). Thus, only BSH is the available nucleophilic thiol that reacts with protein disulfides formed under oxidative stress in *S. aureus* (29). Consistent with this notion, neither cystine nor CoAS disulfide were recognized by Brx at physiological concentrations to oxidize our biosensor *in vitro*. Previous studies identified the OhrR-repressor as redox-controlled under organic peroxide and NaOCl stress by *S*-cysteinylation and *S*-bacillithiolation (6,17). BrxA and BrxB were specific for reduction and reactivation of *S*-bacillithiolated OhrR, but could not regenerate *S*-cysteinylated OhrR (9). These results further support our findings about the specificity of Brx of *S. aureus* for BSSB.

Finally, we studied the changes in the BSH redox potential in *S. aureus* after treatment with sub-lethal doses of different antibiotics to clarify the role of oxidative stress as killing mode for

antibiotics, a controversial debate among microbiologists (16,18). However, we could not detect changes in the BSH redox potential after treatment with rifampicin, fosfomycin, ampicillin, oxacillin, vancomycin, aminoglycosides and fluoroquinolones. Similar to our results, no roGFP2 response was detected by any of these antibiotics in *Salmonella* (39). However, *S. aureus* is resistant to 100 mM H_2O_2 without killing effect and thus, *S. aureus* might be resistant to ROS produced under antibiotics treatment.

In conclusion, we have constructed a novel Brx-roGFP2 biosensor that is highly specific to sense the reduced pool of BSH inside *S. aureus* cells and responds to oxidative stress under infection-like conditions inside macrophages. Using this novel tool, we could demonstrate that commonly used antibiotics do not cause oxidative stress when applied to *S. aureus* and that BSH-deficient mutants have an impaired redox balance and reduced virulence. *S. aureus* is an important human pathogen with new MRSA strains and other multiple antibiotics resistant isolates emerging quickly. This novel probe can be applied in drug-research to screen for new redox-active antibiotics that affect the BSH redox potential in *S. aureus.* In addition, the difference in the ROS detoxification capacity and resistance to host defenses can be monitored across emerging MRSA-isolates to understand the connection between virulence factor expression, antibiotics resistance and the BSH redox potential in *S. aureus*.

INNOVATION

In eukaryotes, glutaredoxin-fused roGFP2 biosensors have been successful applied for dynamic live-imaging of the glutathione redox potential. Here, we have constructed the first genetically encoded bacilliredoxin-fused redox biosensor (Brx-roGFP2) that is specific to measure dynamic changes in the BSH redox potential in the human pathogen *S. aureus* under oxidative stress and infection conditions *in vivo*. Using this biosensor we could confirm that different antibiotics do not cause oxidative stress in *S. aureus*. This Brx-roGFP2 biosensor can be applied to measure redox potential changes across clinical *S. aureus* isolates and to screen for new redox-active antibiotics to treat MRSA infections.

Experimental procedures

Bacterial strains, growth conditions, stress and antibiotics treatments. Bacterial strains, plasmids and primers are listed in Tables S1, S2 and S3. For cloning and genetic manipulation, *Escherichia coli* was cultivated in Luria Bertani (LB) medium. *S. aureus* strains with the pRB473-XylR-Brx-roGFP2 plasmids were cultivated in LB medium with 1% xylose to ensure constitutive expression of the biosensor. For stress experiments, *S. aureus* cells were grown in LB until an optical density at 540 nm (OD_{540}) of 1.0 and transferred to Belitsky minimal medium (BMM) with 1% xylose. The fully reduced control cells were treated with 10 mM DTT and the fully oxidized control was treated with 5 mM diamide for 20 min each, harvested with 10 mM N-ethylmaleimide (NEM) to block the biosensor redox state and transferred to the microplate wells. The samples for stress exposure were transferred to the microplates and different oxidants were injected into the wells of microplates. The Brx-roGFP2 biosensor fluorescence emission was measured at 510 nm after excitation at 405 and 488 nm using the CLARIOstar microplate reader (BMG Labtech) as described below for the *in vitro* measurements. Three biological were performed for each stress experiment.

For the survival assays, *S. aureus* COL wild type and the *bshA* mutant were treated with NaOCl and H_2O_2 at an OD500 of 1.0 in BMM and serial dilutions were plated on LB agar plates and counted for colony forming units (cfu). The survival assays were performed in three biological replicates for each strain.

For the determination of the growth-inhibitory and sub-lethal antibiotics concentrations, *S. aureus* was cultivated in RPMI medium and the antibiotics erythromycin, rifampicin, vancomycin, ciprofloxacin, gentamicin, ampicillin, fosfomycin, lincomycin, linezolid or oxacillin were added at an OD500 of 0.5 to monitor the reduction in growth as described previously (8). The measurements of the biosensor responses after antibiotics treatment were performed in *S. aureus* Brx-roGFP2 cells grown in RPMI-medium and treated with sub-lethal antibiotics doses that reduced the growth rate. Cells were harvested after different times of antibiotics treatment, washed with PBS and blocked with NEM before the microplate reader measurements. Four biological replicates were performed for each antibiotics stress experiment. Sodium hypochlorite, diamide, dithiothreitol (DTT), hydrogen peroxide (H_2O_2, 35% w/v) and antibiotics (erythromycin, rifampicin, vancomycin, ciprofloxacin, gentamicin, ampicillin, fosfomycin, lincomycin, linezolid and oxacillin) were purchased from Sigma Aldrich.

Construction, expression and purification of Brx-roGFP2 in *E. coli.* The Grx-roGFP2 containing plasmid pQE60-Grx1-roGFP2 was obtained from Tobias Dick (11) and used as template for construction of the Brx-roGFP2 fusion. The *brx* gene (*SAUSA300_1321*) was amplified from chromosomal DNA of *S. aureus* USA300 by PCR using primers SAUSA300-1321yphP-FOR-BamHI-NcoI and SAUSA300-1321yphP-REV-SpeI **(Table S3)**, digested with *Bam*HI and *Spe*I and inserted into plasmid pQE60-Grx1-roGFP2 that was digested using the same restriction enzymes to generate plasmid pQE60-Brx-roGFP2. The *brx-roGFP2* sequence was amplified from plasmid pQE60-Brx-roGFP2 by PCR using primers 1321-roGFP2-FOR-NheI and roGFP2-REV-BamHI, digested with *Nhe*I and *BamH*I and sub-cloned into pET11b (Novagen) after digestion by the same enzymes to generate plasmid pET11b-Brx-roGFP2.

For construction of the roGFP2 fusions with the Brx-Cys-to-Ala variants, the Cys residues of the $C_{54}GC_{56}$ active site were replaced by alanine using PCR mutagenesis. For the *brx*C54A mutant, two first-round PCR reactions were performed using primers SAUSA300-1321yphP-FOR-BamHI-NcoI and SAUSA300-1321-yphP-C56A-REV and primers SAUSA300-1321-yphP-C54A-FOR and SAUSA300-1321yphP-REV-SpeI. For the *brx*C56A mutant, two first-round PCRs were performed using primers SAUSA300-1321yphP-FOR-BamHI-NcoI and SAUSA300-1321-yphP-C56A-REV and primers SAUSA300-1321-yphP-C56A-FOR and SAUSA300-1321yphP-REV-SpeI. The two PCR products of each first round PCR reaction were hybridized and subsequently amplified by a second round of PCR using primers SAUSA300-1321yphP-FOR-BamHI-NcoI and SAUSA300-1321yphP-REV-SpeI. The PCR products from the second-round PCRs were then digested with *Bam*HI and *Spe*I and inserted into plasmid pQE60-Grx1-roGFP2 digested with the same enzymes. Subcloning of the Brx-Cys-to-Ala mutant roGFP2 fusions into pET11b was performed as described above.

To construct the *brx*C54A-C56A double mutant, first-round PCR was performed using primers 1321-roGFP2-FOR-NheI and 1321-brx-C54A56A-REV and primers 1321-brx-C54A56A-FOR and SAUSA300-1321yphP-REV-SpeI. Then, the PCR products from first round PCR reactions were fused by PCR using primers 1321-roGFP2-FOR-NheI and SAUSA300-1321yphP-REV-SpeI. The PCR

product from the second-round PCR was then digested with *Nhe*I and *Spe*I and inserted into plasmid pET11b-Brx-roGFP2 digested with the same enzymes.

To construct plasmid pET11b-roGFP2, primers roGFP2-FOR-NheI and roGFP2-REV-BamHI were used to amplify *roGFP2* from plasmid pQE60-Grx1-roGFP2. The PCR product was digested with *Nhe*I and *Bam*HI and inserted into plasmid pET11b digested with the same enzymes. The correct sequences of all plasmid inserts were confirmed by PCR amplification and sequencing.

For Brx-roGFP2 expression, *Escherichia coli* BL21(DE3) plysS containing the pET11-Brx-roGFP2 plasmids was grown in 1 liter LB medium and 1 mM IPTG (isopropyl-β-D-thiogalactopyranoside) was added at the exponential phase (OD600 of 0.8) for 16 h at 25°C. Recombinant His-Brx-roGFP2 and the Brx-Cys-to-Ala mutant roGFP2 fusion proteins were purified using PrepEase His-tagged high-yield purification resin (USB) under native conditions according to the instructions of the manufacturer (USB). The purified proteins were extensively dialyzed against 10 mM Tris-HCl (pH 8.0), 100 mM NaCl, and 50% glycerol and stored at -80°C.

Microplate reader measurements of Brx-roGFP2 and calculation of OxD and E_{BSH}. To study the Brx-roGFP2 response *in vitro*, the purified proteins were reduced with 10 mM DTT for 20 min, desalted with Micro-Bio spin columns (Biorad) and diluted to 1 µM in 100 mM potassium phosphate buffer, pH 7.0. Fluorescence excitation spectra of Brx-roGFP2 were analyzed before and after exposure to the oxidants using the CLARIOstar microplate reader (BMG Labtech) with the Control software version 5.20 R5. Fluorescence excitation spectra were scanned from 360 to 500 nm with a bandwidth of 10 nm, emission was measured at 510nm. Gain setting was adjusted for each excitation maximum. The data were analyzed using the MARS software version 3.10 and exported to Excel. Each *in vitro* measurement was performed in triplicate as indicated in the figure legend. The oxidation degree (OxD) of the biosensor was calculated using the equation (1) as described previously (24,25).

$$OxD = \frac{I405 \times I488_{red} - I405_{red} \times I488}{I405 \times I488_{red} - I405 \times I488_{ox} + I405_{ox} \times I488 - I405_{red} \times I488} \quad (1)$$

The values I405 and I488 are the observed fluorescence excitation intensities at 405 nm and 488 nm, respectively. The values I405red, I488red I405ox and I488ox are the fluorescence excitation intensities at 405 nm and 488 nm of fully reduced and oxidized probes, respectively.

The biosensor redox potential E_{roGFP2} was calculated according to the Nernst equation (2) as described previously (25).

$$E_{roGFP2} = E^{O\prime}_{roGFP2} - \left(\frac{RT}{2F}\right) * \ln\left(\frac{(1-OxD_{roGFP2})}{OxD_{roGFP2}}\right) (2)$$

Because the biosensor equilibrates with the BSH/BSSB redox couple, $E_{BSH} = E_{roGFP2}$.

Construction of Brx-roGFP2 fusions in *S. aureus*. The *brx-roGFP2* sequence was amplified with primers SAUSA300-1321-FOR-BamHI-2 and roGFP2-REV-KpnI-3 and the forward primer also includes the shine-dalgarno sequence of the *brx* gene. The PCR product was digested with *Bam*HI and *Kpn*I and inserted into the pRB473-XylR shuttle vector that was digested using the same enzymes to generate pRB473-XylR-Brx-roGFP2. The plasmids were cloned in *E. coli* DH5α and electroporated into competent cells of *S. aureus* RN4220. The plasmids were transfered into the *S. aureus* target strains COL and USA300 by phage transduction using bacteriophage 80 as described previously (26). *S. aureus* transductants were selected on LB agar with chloramphenicol. The plasmids were isolated and confirmed by PCR and sequencing of the brx-roGFP2 fusion.

Western blot analyses for Brx-roGFP2 expression and BSH-mixed disulfides in *S. aureus*. *S. aureus* strains with Brx-roGFP2 were grown in LB with 1% xylose and harvested at different times during the growth. Cells were washed in Tris-buffer (pH 8.0) with 10 mM NEM, disrupted using the ribolyzer and the protein extract was cleared from cell debris by repeated centrifugation. Protein amounts of 25µg were analyzed by Western blot analysis using mouse-anti-GFP monoclonal antibodies (Tebu Biosciences Cat.-No. 12616810949) as described previously (11). Quantification was performed using the ImageJ software (ver. 1.48, http://imagej.nih.gov) based on a standard curve with purified Brx-roGFP2. The BSH-mixed disulfides were analysed after exposure of *S. aureus* cells to 100 µM NaOCl using non-reducing SDS-PAGE and BSH-specific Western blot analysis with polyclonal rabbit BSH-antibodies as described previously (7).

Confocal laser scanning microscopy of *S. aureus* Brx-roGFP2 strains. *S. aureus* strains with Brx-roGFP2 were exposed to 150 µM of NaOCl, harvested before and after the stress, blocked with NEM

and analyzed by confocal laser scanning microscopy using a ZEISS LSM510meta. The microscope was equipped with a 100× 1.3 M27 EC plan-neofluar oil objective. Fluorescence excitation was performed at 405 and 488 nm and emission was measured using the 505-550nm band pass filter. Cells treated with 10 mM DTT and 5 mM diamide were used as fully reduced and oxidized controls, respectively. The argon/2 and 405 nm laser power were set to 20 and 8%, respectively. The smart gain was 948 V. All setting parameters for the CLSM are listed in **Table S4**. The microscope was calibrated with fully oxidized and reduced *S. aureus* Brx-roGFP2 controls. Quantification of the OxD values was performed from 5 cells each from each sample and the experiments were performed in two biological replicates.

Flow cytometry of *S. aureus* Brx-roGFP2 strains during infection of THP-1 macrophage cell lines. For the infection assays we used the human monocytic leukemia cell line THP-1, which was purchased from the DSMZ strain collection in Heidelberg (DSMZ-no. ACC-16). The cell line was authenticated by multiplex PCR of minisatellite markers which revealed a unique DNA profile and the expression of fusion gene MLL-MLLT3 (MLL-AF9) was confirmed by RT-PCR. Cell cultures were checked for absence of mycoplasma contaminations by PCR on a regular basis. This cell line is not included in the database of commonly misidentified cell lines as maintained by ICLAC. THP-1 cells were cultivated in RPMI-1640 medium with 10% heat inactivated foetal bovine serum (FBS) and seeded in 60 mm cell culture dishes at a density of 4.5×10^6 cells. Differentiation was induced by 100 nM phorbol 12-myristate 13-acetate (PMA) for 24 hours, followed by washing of cells with Hanks balanced salts solution (HBSS) and the addition of fresh medium without PMA. After 24 hours incubation, infection assays of THP-1 macrophages with *S. aureus* were performed as follows. First, *S. aureus* COL cells expressing Brx-roGFP2 were grown in LB with 1% xylose until OD_{540} of 0.5. Bacterial cells were harvested, washed twice and incubated in RPMI-1640 medium. Infection of THP-1 cells with *S. aureus* Brx-roGFP2 was performed at a multiplicity of infection (MOI) of 25 for 1 hour. The infected THP-1 cells were washed twice in PBS-buffer, detached with 0.05% trypsin and 0.02% EDTA, centrifuged and re-suspended in PBS-buffer with 1% FBS. Measurement by flow cytometry was performed on an Attune Acoustic Focusing Cytometer (LifeTechnologies) with excitation at 405

and 488 nm and emission at 515-545 nm. Ten thousand events were gated and the mean fluorescence intensity (MFI) was determined with Attune software V2.1.0 or FlowJo V10.07 (Tree Star). For reduced and oxidized controls, infected THP-1 cells were treated with 20 mM DTT and 150 µM NaOCl, respectively. Infection experiments were performed in 3 biological replicates.

ACKNOWLEDGEMENTS

AUTHOR DISCLOSURE STATEMENT

No competing financial interests exist.

LIST OF ABBREVIATIONS

BMM	belitsky minimal medium
Brx	bacilliredoxin
BSH	bacillithiol
BSSB	bacillithiol disulfide
CA-MRSA	community-aquired MRSA
CFU	colony-forming unit
CLSM	confocal laser scanning microscopy
CoASH	coenzyme A
DTT	dithiothreitol
EDTA	ethylenediaminetetraacetic acid
FBS	Foetal bovine serum
Grx	glutaredoxin
GSH	glutathione
GSSG	oxidized glutathione disulfide
H_2O_2	hydrogen peroxide
HA-MRSA	hospital-acquired MRSA
HBSS	Hanks balanced salts solution
HPLC	high-pressure liquid chromatography
IPTG	isopropyl- β -D-thiogalactopyranoside
LB	Luria Bertani
MFI	mean fluorescence intensity
MOI	multiplicity of infection
MRSA	methicillin-resistant *Staphylococcus aureus*
Mrx1	mycoredoxin1
MSH	mycothiol
MSSM	mycothione or mycothiol disulfide
NADPH	nicotinamide adenine dinucleotide phosphate
NaOCl	sodium hypochlorite
NEM	N-ethylmaleimide
OD_{500}	optical density at 500 nm
OxD	oxidation degree
PBS	phosphate-buffered saline
Rdw	raw dry weight
roGFP	redox-sensitive green fluorescent protein
ROS	reactive oxygen species
Trx	thioredoxin

REFERENCES

1.   Archer GL. Staphylococcus aureus: a well-armed pathogen. *Clin Infect Dis* 26: 1179-81, 1998.
2.   Bhaskar A, Chawla M, Mehta M, Parikh P, Chandra P, Bhave D, Kumar D, Carroll KS, Singh A. Reengineering redox sensitive GFP to measure mycothiol redox potential of Mycobacterium tuberculosis during infection. *PLoS Pathog* 10: e1003902, 2014.
3.   Boucher HW, Corey GR. Epidemiology of methicillin-resistant *Staphylococcus aureus*. *Clin Infect Dis* 46 Suppl 5: S344-9, 2008.
4.   Bratbak G, Dundas I. Bacterial dry matter content and biomass estimations. *Appl Environ Microbiol* 48: 755-7, 1984.
5.   Chen PR, Brugarolas P, He C. Redox signaling in human pathogens. *Antioxid Redox Signal* 14: 1107-18, 2011.
6.   Chi BK, Gronau K, Mader U, Hessling B, Becher D, Antelmann H. S-bacillithiolation protects against hypochlorite stress in Bacillus subtilis as revealed by transcriptomics and redox proteomics. *Mol Cell Proteomics* 10: M111 009506, 2011.
7.   Chi BK, Roberts AA, Huyen TT, Basell K, Becher D, Albrecht D, Hamilton CJ, Antelmann H. S-bacillithiolation protects conserved and essential proteins against hypochlorite stress in firmicutes bacteria. *Antioxid Redox Signal* 18: 1273-95, 2013.
8.   Dorries K, Schlueter R, Lalk M. Impact of antibiotics with various target sites on the metabolome of Staphylococcus aureus. *Antimicrob Agents Chemother* 58: 7151-63, 2014.
9.   Gaballa A, Chi BK, Roberts AA, Becher D, Hamilton CJ, Antelmann H, Helmann JD. Redox regulation in Bacillus subtilis: The bacilliredoxins BrxA(YphP) and BrxB(YqiW) function in de-bacillithiolation of S-bacillithiolated OhrR and MetE. *Antioxid Redox Signal* 21: 357-67, 2014.
10.   Gaballa A, Newton GL, Antelmann H, Parsonage D, Upton H, Rawat M, Claiborne A, Fahey RC, Helmann JD. Biosynthesis and functions of bacillithiol, a major low-molecular-weight thiol in Bacilli. *Proc Natl Acad Sci U S A* 107: 6482-6, 2010.
11.   Gutscher M, Pauleau AL, Marty L, Brach T, Wabnitz GH, Samstag Y, Meyer AJ, Dick TP. Real-time imaging of the intracellular glutathione redox potential. *Nat Methods* 5: 553-9, 2008.
12.   Helmann JD. Bacillithiol, a new player in bacterial redox homeostasis. *Antioxid Redox Signal* 15: 123-33, 2011.
13.   Hillion M, Antelmann H. Thiol-based redox switches in prokaryotes. *Biol Chem*, 2015.
14.   Horsburgh MJ, Clements MO, Crossley H, Ingham E, Foster SJ. PerR controls oxidative stress resistance and iron storage proteins and is required for virulence in Staphylococcus aureus. *Infect Immun* 69: 3744-54, 2001.
15.   Kasozi D, Mohring F, Rahlfs S, Meyer AJ, Becker K. Real-time imaging of the intracellular glutathione redox potential in the malaria parasite Plasmodium falciparum. *PLoS Pathog* 9: e1003782, 2013.
16.   Kohanski MA, Dwyer DJ, Hayete B, Lawrence CA, Collins JJ. A common mechanism of cellular death induced by bactericidal antibiotics. *Cell* 130: 797-810, 2007.
17.   Lee JW, Soonsanga S, Helmann JD. A complex thiolate switch regulates the Bacillus subtilis organic peroxide sensor OhrR. *Proc Natl Acad Sci U S A* 104: 8743-8, 2007.
18.   Liu Y, Imlay JA. Cell death from antibiotics without the involvement of reactive oxygen species. *Science* 339: 1210-3, 2013.
19.   Livermore DM. Antibiotic resistance in staphylococci. *Int J Antimicrob Agents* 16 Suppl 1: S3-10, 2000.
20.   Loi VV, Rossius M, Antelmann H. Redox regulation by reversible protein S-thiolation in bacteria. *Front Microbiol* 6: 187, 2015.
21.   Lowy FD. *Staphylococcus aureus* infections. *N Engl J Med* 339: 520-32, 1998.
22.   Mallett TC, Wallen JR, Karplus PA, Sakai H, Tsukihara T, Claiborne A. Structure of coenzyme A-disulfide reductase from Staphylococcus aureus at 1.54 A resolution. *Biochemistry* 45: 11278-89, 2006.
23.   Meyer AJ, Brach T, Marty L, Kreye S, Rouhier N, Jacquot JP, Hell R. Redox-sensitive GFP in Arabidopsis thaliana is a quantitative biosensor for the redox potential of the cellular glutathione redox buffer. *Plant J* 52: 973-86, 2007.
24.   Meyer AJ, Dick TP. Fluorescent protein-based redox probes. *Antioxid Redox Signal* 13: 621-50, 2010.
25.   Morgan B, Sobotta MC, Dick TP. Measuring E(GSH) and H2O2 with roGFP2-based redox probes. *Free Radic Biol Med* 51: 1943-51, 2011.
26.   Muller M, Reiss S, Schluter R, Mader U, Beyer A, Reiss W, Marles-Wright J, Lewis RJ, Pfortner H, Volker U, Riedel K, Hecker M, Engelmann S, Pane-Farre J. Deletion of membrane-associated Asp23 leads to upregulation of cell wall stress genes in Staphylococcus aureus. *Mol Microbiol* 93: 1259-68, 2014.
27.   Newton GL, Fahey RC, Rawat M. Detoxification of toxins by bacillithiol in Staphylococcus aureus. *Microbiology* 158: 1117-26, 2012.
28.   Newton GL, Rawat M, La Clair JJ, Jothivasan VK, Budiarto T, Hamilton CJ, Claiborne A, Helmann JD, Fahey RC. Bacillithiol is an antioxidant thiol produced in Bacilli. *Nat Chem Biol* 5: 625-7, 2009.
29.   Perera VR, Newton GL, Parnell JM, Komives EA, Pogliano K. Purification and characterization of the Staphylococcus aureus bacillithiol transferase BstA. *Biochim Biophys Acta* 1840: 2851-61, 2014.

30.   Perera VR, Newton GL, Pogliano K. Bacillithiol: a key protective thiol in Staphylococcus aureus. *Expert Rev Anti Infect Ther*: 1-19, 2015.
31.   Perera VR, Newton GL, Pogliano K. Bacillithiol: a key protective thiol in Staphylococcus aureus. *Expert Rev Anti Infect Ther* 13: 1089-107, 2015.
32.   Posada AC, Kolar SL, Dusi RG, Francois P, Roberts AA, Hamilton CJ, Liu GY, Cheung A. Importance of bacillithiol in the oxidative stress response of Staphylococcus aureus. *Infect Immun* 82: 316-32, 2014.
33.   Pother DC, Gierok P, Harms M, Mostertz J, Hochgrafe F, Antelmann H, Hamilton CJ, Borovok I, Lalk M, Aharonowitz Y, Hecker M. Distribution and infection-related functions of bacillithiol in Staphylococcus aureus. *Int J Med Microbiol* 303: 114-23, 2013.
34.   Rajkarnikar A, Strankman A, Duran S, Vargas D, Roberts AA, Barretto K, Upton H, Hamilton CJ, Rawat M. Analysis of mutants disrupted in bacillithiol metabolism in Staphylococcus aureus. *Biochem Biophys Res Commun* 436: 128-33, 2013.
35.   Schwarzlander M, Dick TP, Meye AJ, Morgan B. Dissecting Redox Biology using Fluorescent Protein Sensors. *Antioxid Redox Signal*, 2015.
36.   Sharma SV, Arbach M, Roberts AA, Macdonald CJ, Groom M, Hamilton CJ. Biophysical features of bacillithiol, the glutathione surrogate of Bacillus subtilis and other firmicutes. *Chembiochem* 14: 2160-8, 2013.
37.   Tyagi P, Dharmaraja AT, Bhaskar A, Chakrapani H, Singh A. Mycobacterium tuberculosis has diminished capacity to counteract redox stress induced by elevated levels of endogenous superoxide. *Free Radic Biol Med* 84: 344-54, 2015.
38.   van der Heijden J, Bosman ES, Reynolds LA, Finlay BB. Direct measurement of oxidative and nitrosative stress dynamics in Salmonella inside macrophages. *Proc Natl Acad Sci U S A* 112: 560-5, 2015.
39.   van der Heijden J, Vogt SL, Reynolds LA, Pena-Diaz J, Tupin A, Aussel L, Finlay BB. Exploring the redox balance inside gram-negative bacteria with redox-sensitive GFP. *Free Radic Biol Med* 91: 34-44, 2015.
40.   Weber H, Engelmann S, Becher D, Hecker M. Oxidative stress triggers thiol oxidation in the glyceraldehyde-3-phosphate dehydrogenase of Staphylococcus aureus. *Mol Microbiol* 52: 133-40, 2004.
41.   Winterbourn CC, Kettle AJ. Redox reactions and microbial killing in the neutrophil phagosome. *Antioxid Redox Signal* 18: 642-60, 2013.

FIGURE LEGENDS

Figure 1: Structure of the bacilliredoxin (Brx) SAUSA300_1321 (A), Brx electron pathway (B), principle of the Brx-roGFP2 redox pathway (C) and excitation spectra of Brx-roGFP2 and roGFP2 (A) Bacilliredoxins are Trx-fold proteins of the UPF0403 family with an unusual CGC active site motif. The structure of Brx (SAUSA300_1321) was generated using the software Phyre2 and PyMol **(B)** The *S*-bacillithiolated proteins are reduced by bacilliredoxins (Brx) leading to Brx-SSB formation. Regeneration of Brx requires BSH and the putative NADPH-dependent BSSB reductase YpdA. **(C)** In the Brx-roGFP2 fusion, Brx reacts with BSSB leading to Brx-SSB formation, subsequent transfer of the BSH moiety to the coupled roGFP2 and re-arrangement to the roGFP2 disulfide. The roGFP2 disulfide causes a change of the 405/488 nm excitation ratio. **(D, E)** Purified roGFP2 and Brx-roGFP2 were fully oxidized and reduced with 5 mM diamide and 10 mM DTT, respectively, and the fluorescence excitation spectra were monitored using the microplate reader (n=7-9, $P<0.0001$ in all samples). In all graphs mean values are shown, error bars represent the *s.e.m* and *P*-values were calculated using a Students unpaired two-tailed t-Test by the graph prism software.

Figure 2: Responses of purified Brx-roGFP2, Grx1-roGFP2 and roGFP2 *in vitro* to BSSB, GSSG, MSSM, cystine and CoAS-disulfide. (A,B) Brx-roGFP2 responds specifically to 10 µM and 100 µM BSSB *in vitro* but is non-responsive to GSSG, MSSM, cystine and CoAS-disulfide (n=3, $P<0.0045$ for 10 µM and $P<0.01$ for 100 µM in all samples). **(C)** The roGFP2 probe does not respond to 100µM thiol disulfides (n=3; $P<0.0001$ for BSSB, GSSG, MSSM; $P=0.93$ for cystine). **(D)** The Grx1-roGFP2 fusion shows a specific response to 100µM GSSG, but not to other thiol disulfides (n=3; $P<0.0033$ for all samples). **(E,F)** The response of Brx-roGFP2 to 10µM **(E)** and 100µM BSSB **(F)** was compared to the Brx-Cys mutant proteins BrxAGC-roGFP2, BrxCGA-roGFP2, BrxAGA-roGFP2 and roGFP2 (n=3, $P=0.27$ for 10 µM BSSB BrxAGA; $P<0.0001$ for all others). The results showed that the Brx-roGFP2 response depends on the active site Cys54 of Brx. The thiol disulfides were injected into the microplate wells 90 seconds after the start of measurements and the biosensor response and oxidation degree (OxD) were analyzed using the CLARIOstar microplate reader. In all graphs mean values are shown,

error bars represent the *s.e.m* and *P*-values were calculated using a Students unpaired two-tailed t-Test by the graph prism software.

Figure 3. **Comparison of the Brx-roGFP2 response and expression in *S. aureus* COL and USA300 wild type and *bshA* mutants during the growth. (A,B)** Ratiometric response of Brx-roGFP2 in *S. aureus* COL and USA300 after oxidation of cells by 5 mM diamide and reduction by 10 mM DTT (*n*=7-8; P<0.0001 in all samples). **(C, D)** Expression of Brx-roGFP2 is higher in *S. aureus* COL compared to USA300 during the log phase (*n*=3; P<0.0001 at OD1-1.5) and **(E)** the oxidation degree (OxD) is increased during the stationary phase most strongly in USA300 (*n*=3; P=0.0009 at 6 hours). **(F)** The dynamic range of Brx-roGFP2 is higher in *S. aureus* COL compared to USA300 (*n*=3; P=0.0159 DTT; P=0.0436 Diamide). **(G, H)** The Brx-roGFP2 biosensor is constitutively oxidized in the *S. aureus* COL and USA300 *bshA* mutants in comparison to the wild type strains (*n*=3; P<0.0001 in COL all time points, P<0.01 in USA300 at 4-5.5 hours). Symbols are defined as: ns (P>0.05); * (P≤0.05); ** (P≤0.01); *** (P≤0.001); **** (P≤ 0.0001). The oxidation degree was calculated based on 405/488 nm excitation ratios with emission at 510 nm and related to the fully oxidized and reduced controls as described in the Methods section. In all graphs mean values are shown, error bars represent the *s.e.m* and *P*-values were calculated using a Students unpaired two-tailed t-Test by the graph prism software.

Figure 4: Effect of NaOCl and H_2O_2 on the survival of *S. aureus* wild type and *bshA* mutants and oxidative stress responses of Brx-roGFP2 and Brx Cys-mutant fusions in *S. aureus* COL. (A, B) The *S. aureus* COL and USA300 *bshA* mutants are more sensitive to NaOCl and H_2O_2 stress compared to the wild type as revealed by survival assays (*n*=3; P=0.0473 at 300 mM H_2O_2; P=0.0126 at 30' 150 µM NaOCl). **(C, D)** The Brx-roGFP2 biosensor in *S. aureus* COL is rapidly and reversibly oxidized by sub-lethal concentrations of 1-50 mM H_2O_2 and 10-20 µM NaOCl while higher doses result in constitutive biosensor oxidation (*n*=4; P=0.3186 at 1 mM H_2O_2, P<0.0001 in all other samples). **(E, F)** The response of Brx-roGFP2 and BrxCGA-roGFP2 to H_2O_2 and NaOCl is reversible compared to the active Cys Brx mutant fusions in *S. aureus* COL which is not reversible (*n*=5; P<0.0001 all

samples). In all graphs mean values are shown, error bars represent the *s.e.m* and *P*-values were calculated using a Students unpaired two-tailed t-Test by the graph prism software.

Figure 5: Confocal laser scanning microscopy of *S. aureus* COL Brx-roGFP2 wild type and the *bshA* mutant during NaOCl stress. (A, B) S. *aureus* COL Brx-roGFP2 wild type and *bshA* mutant strains were exposed to 150 µM NaOCl, blocked with NEM and analyzed using CLSM. Cells treated with 10 mM DTT and 5 mM diamide were used as fully reduced and oxidized controls, respectively. Fluorescence emission was measured at 505-550 nm after excitation at 405 nm and 488 nm. Fluorescence intensities at the 488 nm and 405 nm excitation maxima are false-coloured in green and red, respectively and shown in the overlay images and histograms for single cells. The NaOCl-induced oxidation in the wild type and constitutive oxidation of the biosensor in the Δ*bshA* mutant are visualized by the overlay images and the cells are encircled based on the transmitted light image. The histograms show average fluorescence intensities at 405 and 488 nm calculated from 5 representative single cells. **(C)** The average 405/488 nm ratios of the wild type and *bshA* mutant samples were calculated from 5 representative single cells each for the wild type and *bshA* mutant that are marked with bold circles (*n*=5; P=0.001 for control WT/*bshA*). **(D)** For comparison, the 405/488 nm ratios were also calculated from the same *S. aureus* samples using the microplate reader (*n*=3; P=0.0009 for control WT/*bshA*). In all graphs mean values are shown, error bars represent the *s.e.m* and *P*-values were calculated using a Students unpaired two-tailed t-Test by the graph prism software.

Figure 6. Growth curves and OxD of *S. aureus* COL Brx-roGFP2 with sub-lethal concentrations of antibiotics that reduced the growth rate. *S. aureus* was exposed to sub-lethal concentrations of antibiotics at an OD500 of 0.5 and the OxD of Brx-roGFP2 was monitored in treated and untreated cells (*n*=4; P>0.05 for OxD control/antibiotics treatment in all samples). The following sub-lethal antibiotics were used: 0.1 µM erythromycin, 0.1 µM rifampicin, 5 µM vancomycin, 30 µM ciprofloxacin, 0.1 µM gentamycin, 10 µM ampicillin, 50 mM fosfomycin, 5 µM lincomycin, 2 µg/ml linezolid, 2 mM oxacillin. There was no increased oxidation by antibiotics in *S. aureus*. In all graphs mean values are

shown, error bars represent the *s.e.m* and *P*-values were calculated using a Students unpaired two-tailed t-Test by the graph prism software.
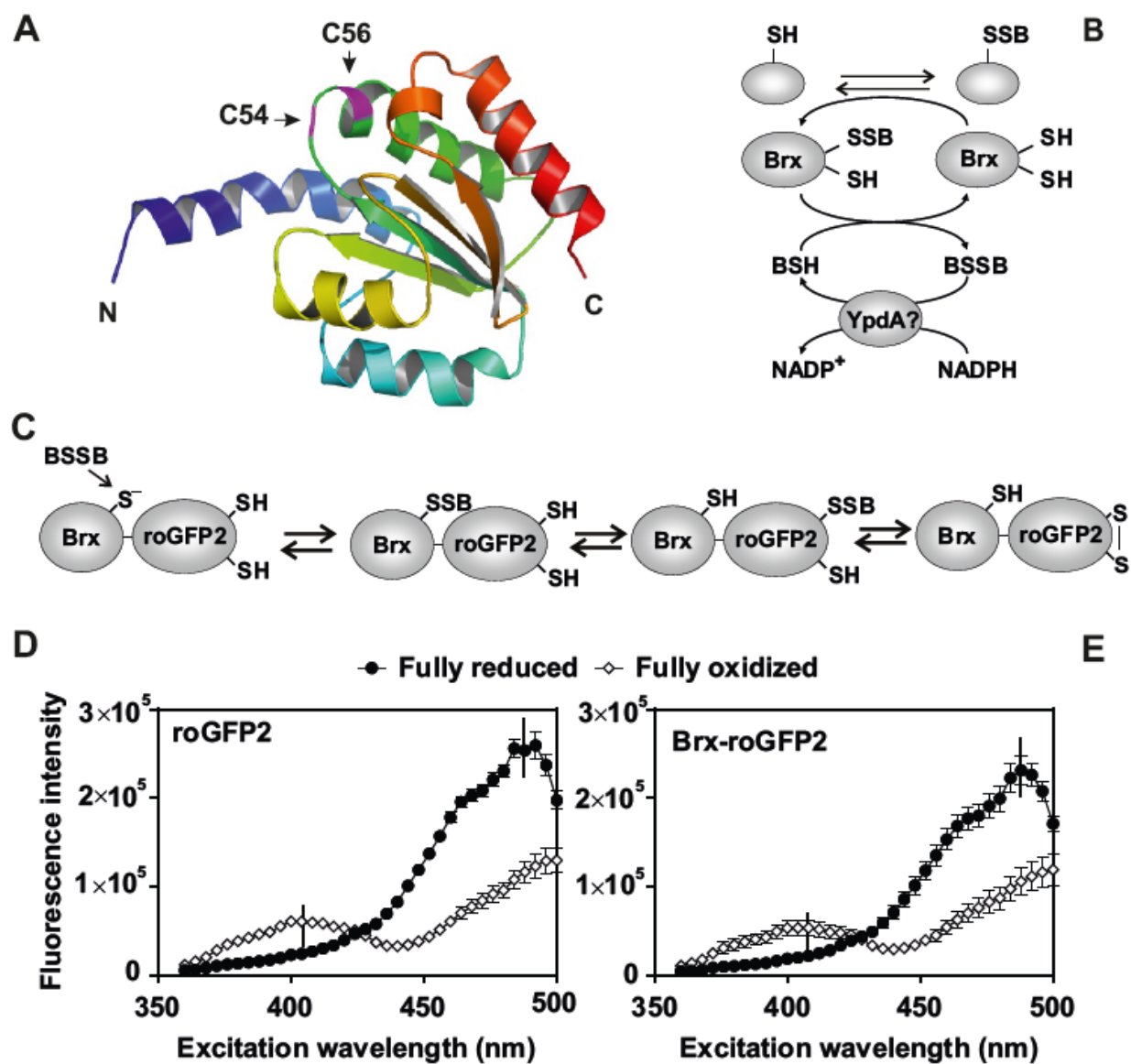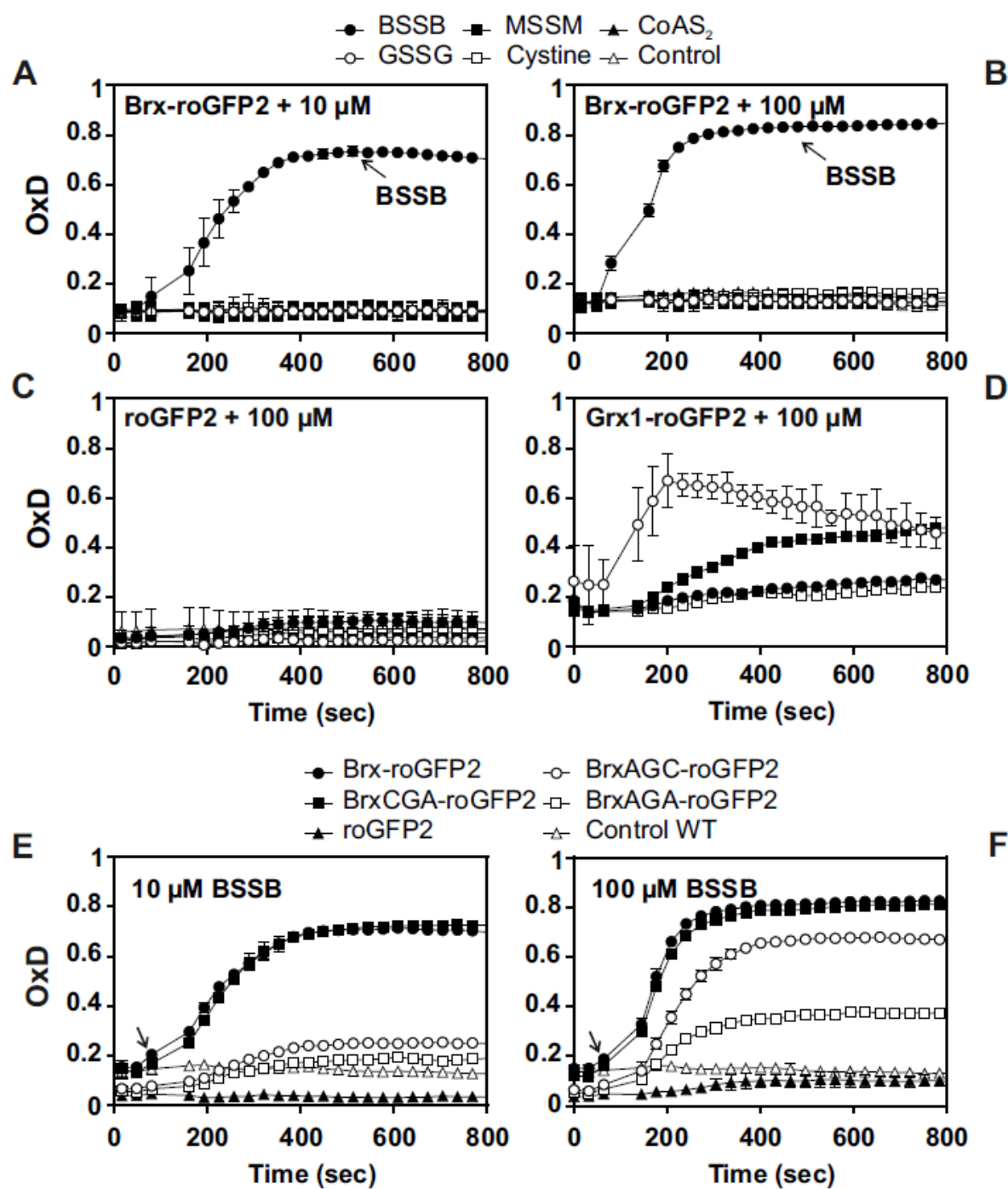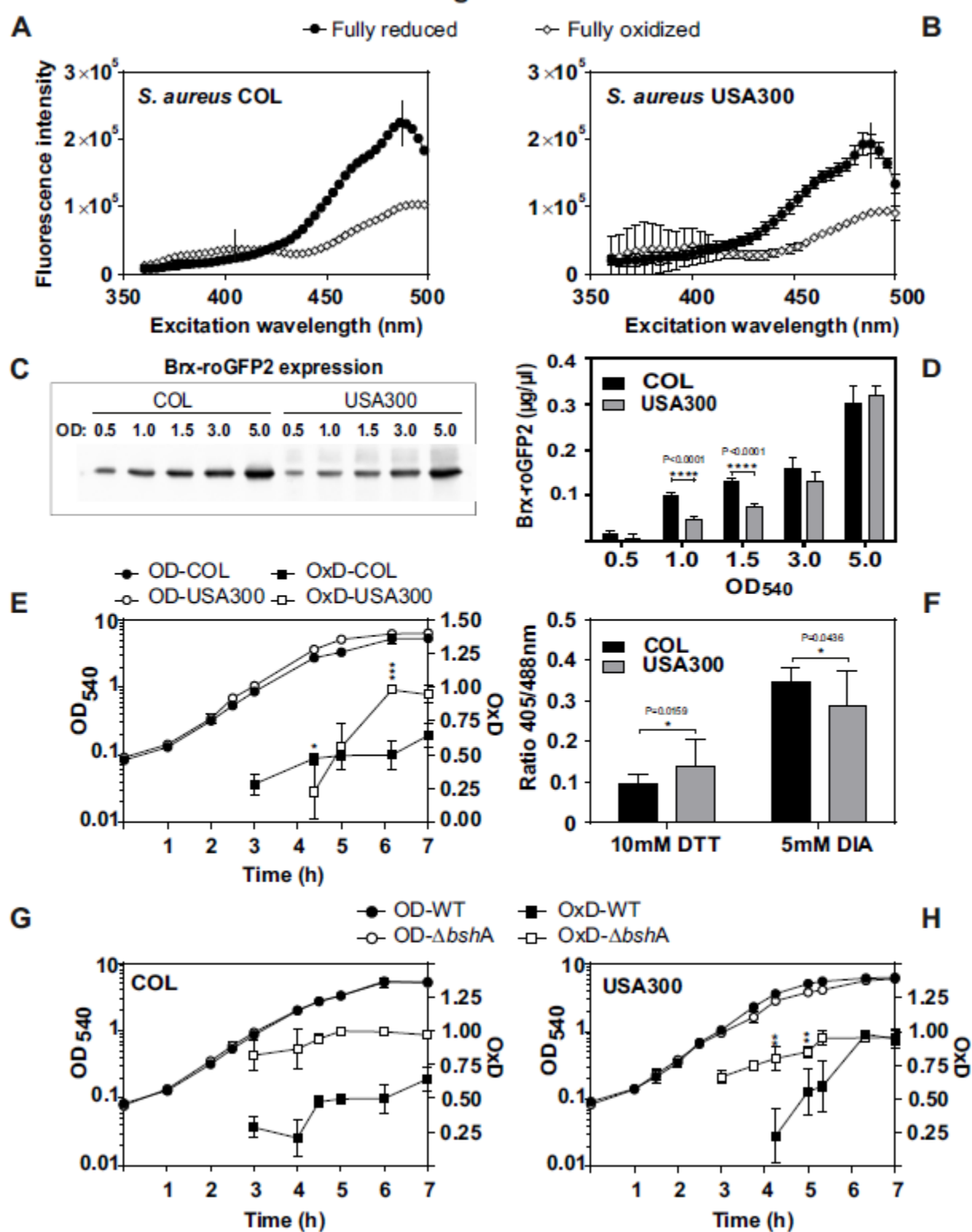
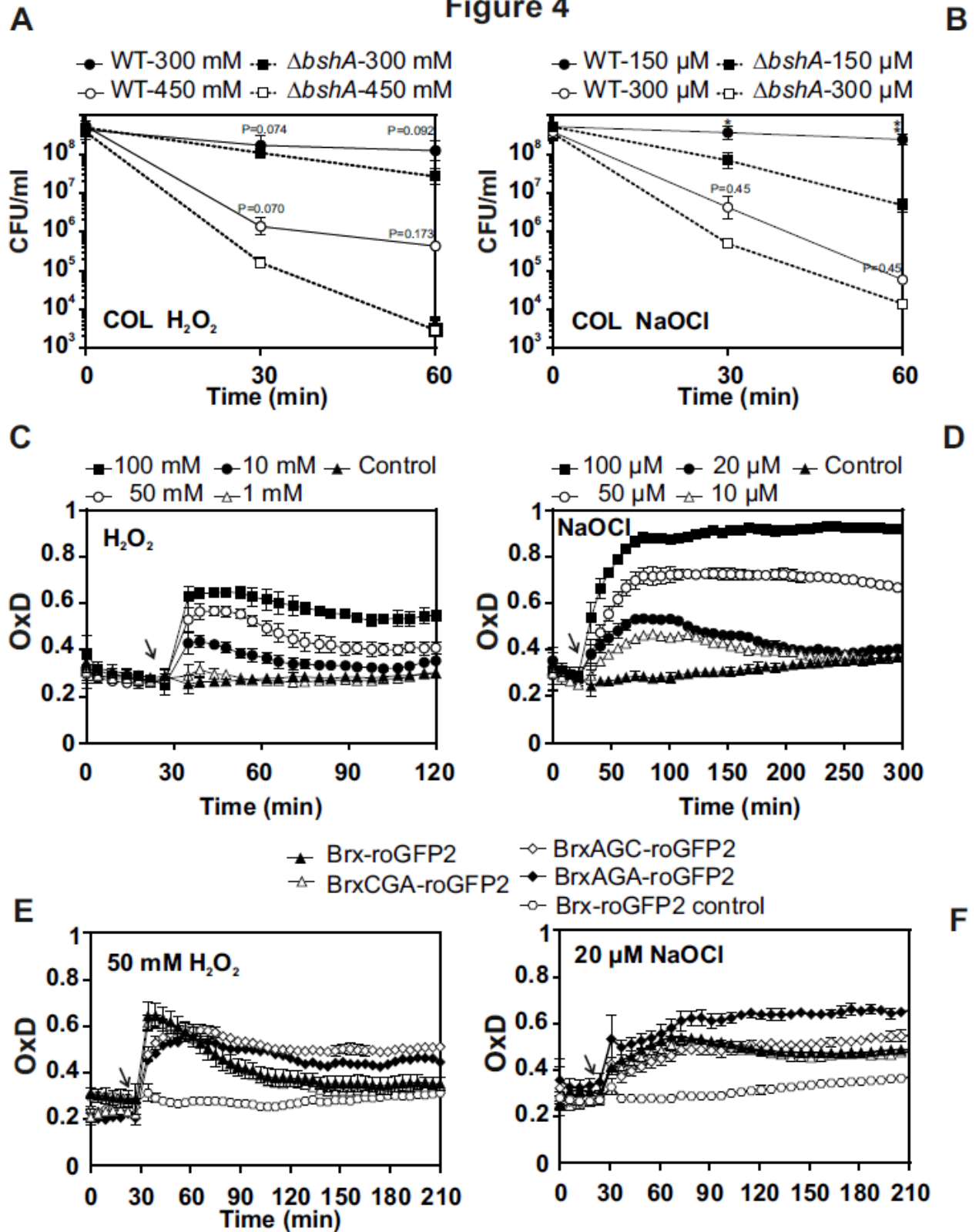# Figure 1

Figure 2

Figure 3

Figure 4

Figure 5

Figure 6

Legend: OD-Control, OxD-Control, OD-antibiotics, OxD-antibiotics

A. 0.1 µM erythromycin
B. 0.1 µM rifampicin
C. 5 µM vancomycin
D. 30 µM ciprofloxacin
E. 0.1 µg/ml gentamicin
F. 10 µM ampicillin
G. 50 mM fosfomycin
H. 5 µM lincomycin
I. 2 µg/ml linezolid
J. 2 mM oxacillin